Prediction of hydraulic jump characteristics in a closed conduit using numerical and analytical methods

Ehsan Maryami[1], Reza Mohammadpour[2*], Mohammad Karim Beirami [1,3], Ali Torabi Haghighi[4]

[1]*Department of Civil Engineering, Islamic Azad University, Estahban Branch, Fars, Iran.*

[2*]*Assistant professor Department of Civil Engineering, Islamic Azad University, Estahban Branch, Fars, Iran. (Email:reza564@gmail.com)*

[3]*Associate Professor, Isfahan Univ. of Technology (IUT), Isfahan, Iran*

[4] *Associate Professor, Water, Energy and Environmental Engineering Research Unit, University of Oulu, Oulu, Finland*

Abstract

The hydraulic jump is an economical alternative to dissipate energy in the conduit and to reduce erosion at the culvert outlet. In the literature, very limited studies have been reported on the performance of hydraulic jump in a closed conduit. The innovation of this research is to employ a numerical method for the estimation of the hydraulic jump characteristics in a closed conduit with different positive slopes (S_0). The analytical method was used to develop several equations for hydraulic jump and the provided results were compared with the numerical method. The results indicate that the numerical method predicts the flow depth ratio after conduit with higher accuracy (error less than 5%) in comparison to the analytical method (error less than 10%). Furthermore, in the slope of 0.00, the energy loss increases by 16% with increasing the Froude number from 4.617 to 5.562 while this value is 23% and 22% for slopes of 0.01 and 0.02, respectively. Finally, several equations were developed for the prediction of hydraulic jump characteristics in terms of Fr_1, S_0, and conduit depth (D).

Keywords: Conduit; Hydraulic jump; positive slope; Numerical model; Analytical method

Introduction

The hydraulic jump is known as a rapid change of supercritical flow into subcritical which always occurs with considerable energy dissipation and turbulence. In this phenomenon, the energy loss increases with increasing the water level at downstream (Chow, 1959) and it can be used to reduce flow energy downstream hydraulic structure (Altalib et al., 2019). At the culvert outlet as well as closed conduit, the supercritical flow is the main reason for local scour and sediment erosion. One of the best ways to protect the channel against erosion is to dissipate the energy within the closed conduit. Therefore, the hydraulic jump has been often used as an economical alternative to dissipate energy in conduit and culvert design (Hotchkiss et al., 2005). The behavior of hydraulic jump in closed conduits (such as culverts) with a free surface is similar to open-channel. If flow depth increases at downstream, it may completely fill the conduit and leads to create a pressurized flow which is known as incomplete hydraulic jump (Caric 1977; Hager, 1999; Hotchkiss et al., 2003; Montes, 1998). The length and height of hydraulic jump are necessary to be predicted to control its location (Thompson and Kilgore 2006). It should be mentioned that the length of the hydraulic jump is depended on the hydraulic jump height, while its location depends on hydraulic conditions.

The channel slope is a key factor that can deeply change hydraulic jump properties (Palermo and Pagliara, 2018). Several investigations have been carried out to analyze the hydraulic jump in an open-channel with the smooth sloping floor (Kawagoshi and Hager 1990, and Ohtsu and Yasuda 1991; Kindsvarter, 1944; Pagliara and Palermo 2015, Wang et al. 2021). Hager (1988) investigated the hydraulic jump in a rectangular channel with a slope at the upstream and a horizontal bed at the downstream. He reported several details related to the hydraulic jump efficiency, the sequent depths, the horizontal bottom force component, and the length characteristics. Based on the momentum equation, Beirami, and Chamani, (2006) recommended a method to predict the sequent depth of hydraulic jumps in sloping channels. They showed that the negative slope of the basin reduces the sequent depth ratio, while a positive slope increases the sequent depth ratio. Kumar and Lodhi (2015) investigated the hydraulic jump characteristics in a channel with a positive slope and rough floor. They showed that the channel slope significantly impacts hydraulic jump characteristics. A good agreement was observed between the experimental data and proposed equations for the length of the roller, the sequent depth ratio and relative energy loss in the hydraulic jump. Abdel-Mageed (2015) investigated the effect of a positive slope on characteristics of the hydraulic jump downstream of the vertical gate. Based on experimental data, several equations have been developed for the estimation of sequent depth ratio, length and distance of the hydraulic jump. Parsamehr et al. (2017) studied characteristics of the hydraulic jump in a channel with an adverse slope and rough bed. They reported that relative length and sequent depth ratio decreases with increasing the adverse slope and height of roughness elements. Palermo and Pagliara (2017) and (2018) showed that bed roughness contributes to modify hydraulic jump characteristics and the dissipative process on sloping beds. Pourabdollah et al. (2019) employed experimental and analytical methods to study hydraulic jump characteristics on different adverse slopes, bed roughness, and positive step heights. The results showed that the decrease in the sequent depth ratio and the increase in the relative energy loss were 33 and 27.41% more than those in the classic jump, respectively. Furthermore, to estimate the sequent depth ratio, two new analytical solutions were developed using the momentum equation. Kumar et al. (2021) experimentally investigated the characteristics of hydraulic jumps formed on rough sloping channel beds under different flow conditions. A rectangular flume with different bed roughness and slope was used to determine the sequent depth of hydraulic jump. New equations were proposed for parameters of the hydraulic jump with high accuracy.

Smith and Chen (1989) studied the hydraulic jump in a closed conduit with steep slopes (up to 30%). A wide range of Froude numbers and slopes were chosen in this study. Since there were too many unknowns, they could not theoretically develop a direct solution for jump length in conduit. Godley (2002) was measured the free surface flow in partially filled closed conduits. He showed that selection of an appropriate instrument for a particular site is dependent on the precise requirements and conditions at each site. Raikar et al. (2010) employed regression method to compute the normal and critical depths for an egg-shaped conduit section. They showed that a good accuracy was observed between observed values and fundamental equations. Lowe et al. (2011) determined the sequent depths in a closed conduit using the theoretical method. The momentum equation was used to estimate the sequent depth in four commonly shaped conduits: rectangular, circular, elliptical, and pipe arch. They reported that the suggested solutions may be used to predict the size and location of hydraulic jumps in the closed conduit. Reshwan (2013) used the momentum principle to develop relations for the hydraulic jump in the semicircular open channel. He showed that the conjugate and initial depth could be expressed as a function of the critical depth. The design curve was recommended for the Froude number and ratio of conjugate depth.

Chiew and Emadzadeh (2017) experimentally investigated the free surface and pressure fluctuations of hydraulic jump in a closed conduit. They measured high-pressure fluctuations at the downstream end of closed-conduit jumps. Wang et al. (2018) presented a method of mass flow measurement based on swirl motion in circular conduits. They reported that this method provide an easy way to be standardized the data. Wang and Li (2018) used a circular pipe of the steep slope to investigate the hydraulic jump and flow behavior. The momentum principle was employed to formulate the hydraulic jump in the circular pipe. Different results were reported in their studies such as initial versus sequent depth of the hydraulic jumps and slope-filling ratio space between flow-choking and choking-free zones.

The numerical model and soft computing techniques can be considered as an economic and low-cost method to investigate a wide range of hydraulic and complex problems (Mohammadpour et al. 2013, 2014, 2017, 2018; Pham et al. 2020, Harun et al. 2021). Zounemat-Kermani et al. (2017) used gene expression programming (GEP) and decision tree methods to estimate aeration coefficient in outlet conduits of dams. The GEP provides better prediction for air demand and the aeration coefficient in comparison to other models. Recently, computational Fluid Dynamics (CFD) has been used to study the different characteristics of the hydraulic jump (Chippada et al .1994; Abbaspour et al. 2009; Carvalho et al. 2008; Madsen et al. 2005; Bayon and Lopez-Jimenez 2015; Witt et al. 2015; De Padova et al. 2010, 2018). The mechanism of a circular hydraulic jump was numerically investigated by Yokoi and Xiao (1999), Teymourtash and Khavari (2011) and Passandideh-Fard et al. (2011). Mohammadpour et al. (2013) reported that the accuracy of numerical modeling is dependent on the turbulence model. Furthermore, the k –ε can be used as an accurate turbulence method for the simulation of hydraulic problems with the free surface. Azimi et al. (2014) simulated free surface and velocity field in a circular channel in supercritical conditions. The Volume Of Fluid (VOF) and RNG k-ε techniques were used to simulate the free surface and turbulence, respectively. Comparison between the numerical simulation and experimental results indicated high accuracy of the CFD model in modelling of flow characteristics in the circular channel. Bayon et al. (2016) employed OpenFOAM and FLOW-3D to simulate a hydraulic jump in the channel with a low Reynolds number. The OpenFOAM is a source platform containing several C++ libraries and applications which can numerically solve continuum mechanics problems (Weller et al., 1998) and the FLOW-3D is a commercial software package. They used structural mesh, VOF and RNG k-ε technique in both codes. A comparison between numerical and experimental data in the channel with a low Reynolds number showed that the models are successfully able to predict the energy dissipation of hydraulic jump. Celik et al. (2008) reported that FLOW-3D software with coarser meshes can converge fasters than OpenFOAM code. A summarize of different turbulence models used to study the hydraulic jump is shown in Table 1. As shown in this table, the Reynolds-Averaged Navier Stokes (RANS) and k –ε methods are the most widely used for the simulation of hydraulic jump. Najafzadeh (2019) utilized three numerical models based on evolutionary computing to evaluate the conjugate depths of the hydraulic jump in the circular pipes. The performance of the model tree (MT) indicated an accurate prediction of conjugate depths in comparison with other artificial intelligence (AI) models and empirical equations. Moreover, the linear MT equation had a more convenient application in comparison with empirical equations. Hafnaoui and Debabeche (2020) simulated the location and displacement of the hydraulic jump in a rectangular channel using 2D numerical modeling. A comparison between experimental data and numerical modeling showed that numerical simulation satisfactorily predicted the hydraulic jump location. Li et al. (2020) employed Flow-3D software to numerically simulate the flow pattern of three cylindrical mobile flumes, including circular cylinder, elliptical cylinder and V-tailed cylinder mobile flumes. They used U-shaped channels to analysis the hydraulic characteristics including back- water height, energy. Finally, the cylindrical mobile flume was recommended to make the upstream water flow more stable. Baharvand et al. (2020) developed a non-linear regression algorithm to predict the sequent depth ratio of hydraulic jumps over a smooth and rough bed. They have used machine learning techniques to check the accuracy of the proposed algorithm. It is shown that the proposed model predicted the hydraulic jump sequent depth ratio more accurately compared to the linear regression techniques. However, there are few equations to predict the conjugate depth of hydraulic jump in circular pipes (Najafzadeh, 2019). In the literature, very limited studies have been reported on the performance of hydraulic jump in a closed conduit. Therefore, a comprehensive study is necessary to determine the hydraulic jump characteristics in a closed conduit with different slopes.

In this study, the analytical and numerical methods were employed to study hydraulic jump parameters in a closed conduit with different slopes. The hydraulic jump parameters such as secondary depth, jump length, energy dissipation and the flow depth immediately after conduit were investigated using the numerical method and the provided results were compared with suggested analytical equations. In the analytical method, the hydraulic jump parameters were calculated using momentum and energy equations in different sections and then the provided results are compared with numerical and experimental data. Finally, a comparison between numerical, analytical and experimental results was conducted to investigate the accuracy of each method.

Experimental data

The numerical modeling was employed to investigate the hydraulic jumps in sloping rectangular closed conduits. The experimental results provided by Ezzeldin et al. (2000a) were used to simulate the numerical modeling. They have conducted the experimental tests in a flume with the dimension of, 3.0 m long, the width of 10 cm and 31 cm deep. An initial supercritical depth (d_1) was adjusted using the control gate at upstream of the conduit. Another gate was installed downstream of the flume to control the tail-water outlet depth (D_t) and form the hydraulic jump at a certain location of the conduit. Different parameters of the hydraulic jump in the conduit are shown in Figure 1a and Table 2.

Five different depths were chosen for conduit for experiments including 6, 7, 8, 9 and 10 cm (Figure 1a). A horizontal conduit (S_0=0.00) and two positive slopes of 0.01 and 0.02, as well as different Froude numbers (Fr) between 4 and 5, were used in the tests. The experimental data is shown in Table 3.

Numerical modeling

In this study, the FLUENT package was used to solve the Navier-Stokes equations which can be expressed as:

$$\frac{\partial}{\partial t}(\rho) + \nabla.(\rho\,\vec{v}) = 0 \tag{1}$$

$$\frac{\partial}{\partial t}(\rho\,\vec{v}) + \nabla.(\vec{v}\,\vec{v}) = -\nabla p - \nabla.\left[\mu\left(\nabla\,\vec{v} + \nabla\,\vec{v}^{\,T}\right)\right] + \rho\,\vec{g} + \vec{F} \tag{2}$$

where $\vec{v}$ is velocity; p is pressure; ρ is the fluid density; μ is fluid viscosity; t is time; g is gravity acceleration and $\vec{F}$ is the body force.

The control volume technique, implicit method, Semi- Implicit algorithm (SIMPLE), the first-order upwind and the first-order Power-Law scheme were employed to predict the hydraulic jump in conduit.

3.1. Free surface

The model of conduit with water and a region of air on the top, the two-phase model, was simulated using the volume of fluid (VOF) method. The VOF equation, which can be expressed using Equation (3), was solved by the control volume technique. It should be noted that the value of $\alpha_w=0.5$ indicates the free surface of the flow (Dargahi 2006).

$$\frac{\partial \alpha_w}{\partial t} + \nabla.(v.\alpha_w) = 0 \tag{3}$$

where and v = kinematic viscosity of water and α_w = water volume fraction.

3.2. Turbulence Model

The *k-ε* turbulence is the simplest model which is recommended by Younus and Chaudhry (1994). Viti et al. (2018) reported that the k-ε is the most widely-used engineering turbulence model for industrial applications because of its robustness and reasonable accuracy for a wide range of flows. Bayon et al. (2019) investigated the effect of the RANS turbulence model in the hydraulic jump. They showed that the most accurate turbulence model is the RNG k-ε to simulate hydraulic jumps. The *k-ε* model solves two different transport equations that result in the determination of the turbulent kinetic energy and its dissipation rate. The 3-D form of governing equations for the *k-ε* model can be expressed as (Launder and Spalding 1972):

$$\frac{\partial}{\partial t}(\rho k) + \frac{\partial}{\partial x}(\rho k u) = \frac{\partial}{\partial x}\left[\left(\mu + \frac{\mu_t}{\sigma_k}\right)\frac{\partial k}{\partial x}\right] + G_k + G_b - \rho\varepsilon - Y_M \tag{4}$$

$$\frac{\partial}{\partial t}(\rho\varepsilon)+\frac{\partial}{\partial x}(\rho\varepsilon u)=\frac{\partial}{\partial x}\left[\left(\mu+\frac{\mu_t}{\sigma_\varepsilon}\right)\frac{\partial\varepsilon}{\partial x}\right]+C_{1\varepsilon}\frac{\varepsilon}{k}(G_k+C_{3\varepsilon}G_b)-C_{2\varepsilon}\rho\frac{\varepsilon^2}{k} \qquad (5)$$

The μ_t can be written as:

$$\mu_t=\rho C_\mu\frac{k^2}{\varepsilon} \qquad (6)$$

where G_b and G_k are the generation of the turbulent kinetic energy due to buoyancy and mean velocity gradients respectively; Y_M is the contribution of the fluctuating dilatation incompressible turbulence to the overall dissipation rate; $C_{1\varepsilon}$, $C_{2\varepsilon}$, and $C_{3\varepsilon}$ are constants and equal to 1.44, 1.92 and 0.09 respectively; σ_k and σ_ε are the turbulent Prandtl Numbers for k and ε equal to 1.0 and 1.3 respectively.

3.3. Boundary conditions

The channel dimension and the boundary conditions are shown in Figure 1b and Figure 2a, respectively. To simulate hydraulic jump in the conduit, the uniform velocity with the flow depth is imposed on the inlet. Since the air is located at the upper surface of the channel, symmetry was employed for this boundary. The symmetry boundary condition applies the zero gradient condition which is suitable for the upper surface. The water level at the channel outlet is not predictable then the pressure outlet was selected for the channel outlet. At the solid boundary and the walls such as the bed, the no-slip boundary (wall) was employed to set a value of zero for velocity. Moreover, to estimate the effect of walls on the flow, the empirical wall functions were used as a standard wall function (Launder and Spalding, 1974). The meshes are shown in Figure 2b.

Analytical modeling of hydraulic jump

Three equations of momentum, continuity, and energy can be used to determine the analytical equations in a sloping closed conduit. In the literature, there are different researches about the analytical model of hydraulic jump (Haindl 1957; Hsu et al., 1980; Hager, 1992; Chanson, 2015). As shown in Figure 1a, four sections were selected to develop equations. The location of section 2 is considered at the end of the closed conduit and before the open channel. In this location, the top of the conduit limits the sequent depth of the hydraulic jump and a big energy loss occurs in this location. Since the energy loss is unknown between sections (1) and (2) as well as (3) and (4), then the momentum equation was used in these sections, the results could be expressed as:

1- Momentum equation between sections (1) and (2):

$$\frac{1}{2}d_1{}^2\times b\times\cos^2\theta-\left(d_2-\frac{D}{2}\right)\times b\times D\times\cos^2\theta+\frac{1}{2}\ S_0\times L_{(1-2)}\times b\times(d_1\cos\theta\ +d_2\cos\theta\ ) \tag{7}$$

$$=\frac{Q^2}{g}\left(\frac{\cos\ \theta}{D\times b}-\frac{\cos\ \theta}{d_1\times b}\right)$$

2- Since the energy loss is a coefficient of kinetic energy, then in Eq. (8), the energy loss was considered as $K\left(\frac{V_3{}^2}{2g}-\frac{V_2{}^2}{2g}\right)$ which is a coefficient of kinetic energy between sections (2) and (3), Energy equation between sections (2) and (3):

$$d_2\cos\ \theta+\frac{V_2{}^2}{2g}+S_0\times L_{(2-3)}=d_3\cos\ \theta+\frac{V_3{}^2}{2g}+K\left(\frac{V_3{}^2}{2g}-\frac{V_2{}^2}{2g}\right) \tag{8}$$

3- Momentum equation between sections (3) and (4):

$$\frac{1}{2} d_3{}^2\cos^2\theta \times b-\frac{1}{2} D_t{}^2\cos^2\theta \times b+\frac{1}{2}\ S_0\times L_{(3-4)}\times(d_3\cos\theta+D_t\cos\theta)\times b=\frac{Q^2}{g}\left(\frac{\cos\theta}{b\times D_t}-\frac{\cos\theta}{b\times d_3}\right) \tag{9}$$

As shown in Figure 3, the energy loss between sections (1) and (2) can be determined using the following equations:

$$\Delta E=(Z_1+d_1\cos\theta+\alpha_1 V_1{}^2/2g)-(Z_2+d_2\cos\theta+\alpha_2 V_2{}^2/2g) \tag{10}$$

$$E_1=d_1\cos\theta+\alpha_1\frac{V_1{}^2}{2g}=d_1\cos\theta+\alpha_1\frac{Q^2}{2gA_1{}^2} \tag{11}$$

$$E_2=d_2\cos\theta+\alpha_2\frac{V_2{}^2}{2g}=d_2\cos\theta+\alpha_2\frac{Q^2}{2\,g\,A_2{}^2} \tag{12}$$

$$A_2=b\times D,\qquad A_1=b\times d_1 \tag{13}$$

$$\Delta E=(E_1+\Delta z)-E_2 \tag{14}$$

$$\frac{\Delta E}{E_1}=\text{Energy loss ratio} \tag{15}$$

As shown in Figure 1a, the length of the hydraulic jump (Lr) between sections (1) and (2) is calculated using the following equation (Beirami and Chamani, 2010):

$$Lr=d_1\cos\theta\times\left(\frac{d_2}{d_1}-1\right)\times(Fr_1{}^2+Fr_2{}^2-2)/(2SF-2S_0) \tag{16}$$

$$SF=0.\,255\times(Fr_1{}^{2.\,1}-Fr_2) \tag{17}$$

$$Fr_1=\left(\frac{Q^2\times b}{g\times A_1{}^3\times\cos\theta}\right)^{0.5} \tag{18}$$

$$Fr_2=\left(\frac{Q^2\times b}{g\times A_2{}^3\times\cos\ \theta}\right)^{0.5} \tag{19}$$

The water depth at section (2) (d_2) is expressed using the following equations:

$$d_2=\frac{K_2\text{-}K_1}{K_3} \tag{20}$$

$$K_1=\frac{Q^2}{\left(g\times b^2\right)\times\left(\frac{1}{(D\text{-}1)\times d_1}\right)} \tag{21}$$

$$K_2=\frac{1}{2}*d_1{}^2\times\cos\ \theta+\frac{1}{2}\times D^2\times\cos\ \theta+\frac{4}{4\times S_0\times L_r\times d_1} \tag{22}$$

$$K_3=D\times\cos\ \theta\ \text{-}\frac{4}{4\times S_0\times L_r} \tag{23}$$

The water depth at section (3) was calculated using the energy equation between sections (2) and (3). Finally, the following equation was suggested for (d_3):

$$d_2\times\cos\ \theta+HV_2+S_0\times L_D=d_3\times\cos\ \theta+HV_3\ \text{-}K(HV_3\text{-}HV_2);\ K=0.86 \tag{24}$$

$$d_3=(S_0\times L_D+d_2\times\cos\ \theta+HV_2\text{-}HV_3\text{-}0.86(HV_3\text{-}HV_2))/\cos\ \theta \tag{25}$$

$$HV_2=\frac{Q^2}{2\times g\times b^2\times D^2} \tag{26}$$

$$HV_3=\frac{Q^2}{2\times g\times b^2\times D^2\times Cc^2} \tag{27}$$

The water depth at section (4) (d_4) can be calculated using the following equations:

$$d_4=[(S_2\text{-}S_1)/S_3]^{0.5} \tag{28}$$

$$S_1=\left(\frac{Q^2}{gb^2}\right)\times\left(\frac{\cos\ \theta}{d_4}-\frac{\cos\ \theta}{D*Cc}\right) \tag{29}$$

$$S_2=\frac{1}{2}d_3{}^2\times\cos\ \theta\ ^2+\frac{1}{2}S_0\times L_{3-4}\times(d_3+d_4) \tag{30}$$

$$S_3=\frac{1}{2}\cos\theta\ ^2 \tag{31}$$

Results and Discussion

Figure 4 shows the hydraulic jump in a closed conduit using the numerical model. The results of numerical modeling for three positive slopes of 0.00, 0.01and 0.02 are shown in Table 4. The results including different depths of hydraulic jump such as d_1, d_2, d_3 and d_4 as well as L_r (Figure 1a and Table 2). The range of Froude number was chosen between 4.0 and 6.0 and the ratio of d_4/d_1 was selected for validation. The experimental results given by Ezzeldin et al. (2000a) were used to evaluate the accuracy of numerical modeling. A comparison between numerical modeling and experimental data in terms of d_4/d_1 is shown in Table 5. In all cases, the error percentage is less than 5%. However, the accuracy of numerical modeling decreases with increasing the Froude number, except test No. 9. The bar chart, residual and scatter graph related to this table are shown in Figure 5. A good agreement can be observed between numerical modeling and experimental data. It can be concluded that the VOF method can predict the flow depth in hydraulic jump with high accuracy and low error (R^2=0.991, RMSE=0.077).

Table 6 shows the results of the analytical method in conduit with a different positive slope. The results including different depths in the conduit (d_1, d_2, d_3 and d_4) and hydraulic jump length (L_r) with different Froude numbers between 4.0 and 6.0. The ratio of d_4/d_1 and similar experimental data were chosen to validate the recommended analytical equations. A comparison between the analytical method and experimental data is shown in Table 5. The percentage of error in all cases is less than 10%. As shown in Figure 6, the recommended analytical equation can predict the depth ratio (d_4/d_1) with good accuracy (R^2=0.881, RMSE=0.291). The results indicate that the accuracy of numerical modeling is higher than the analytical method to forecast the flow depth in conduit.

Variation of the flow depth after the hydraulic jump (d_2 and d_3) in terms of the Froude number for both analytical and numerical methods is shown in Figure 7. In a closed conduit, similar to hydraulic jump in an open channel, the flow depth increases with increasing the Froude number. Table 7 shows that the average increase of both d_2/d_1 and d_3/d_1 is around 15% with increasing the slope from 0.00 to 0.02 and Froude number from 4.61 to 5.56. As shown in Table 5, similar results can be observed for the ratio of d_4/d_1. For instant, in numerical modeling with increasing Froude number from 4.617 to 5.562, depth ratio (d_4/d_1) increases from 5.56 to 7.01, respectively. The results indicate that both analytical and numerical methods predict d_3 close to each other while there is a large difference between these methods in predicting d_2. It can be due to the limitation of closed conduits for hydraulic jump formation. Furthermore, in all cases, the prediction of flow depth by the analytical method is less than the numerical method.

The variation of hydraulic jump length in the conduit is shown in Figure 8. In all slopes, the length of the hydraulic jump (L_r/d_1) increases with increasing the Froude number (Figure 8a). A similar trend was observed between the presented study and the results presented by Rajaratnam and Subramanya (1968) as well as Abdel-Mageed (2015). The difference between results can be due to the kind of channels and experiments. It should be noted that Rajaratnam and Subramanian (1968) used a smooth and horizontal rectangular channel while Abdel-Mageed (2015) employed a sloped rectangular channel. As shown in Figure 8b, on the same slope, the length of the hydraulic jump increases with increasing Froude number. For instant, in numerical modeling with S0=0.01 the value of L_r/d_1 increases from 8.39 to 9.65 with increasing Froude number from 4.617 to 5.037, respectively. The difference between the results of the presented study and those reported by Abdel-Mageed (2015) is due to the hydraulic jump in closed conduit and rectangular channel. The previous researchers reported that the hydraulic jump length in the rectangular channel is a function of channel slope and the Froude number (Rajaratnam, 1967; RangaRaju, 1993; Kumar and Lodhi, 2016). Figure 8b shows that in the closed conduit as well as rectangular channel, the hydraulic jump length is a function of both mentioned parameters and the length of hydraulic jump increases with increasing the slope and Froude number.

Both numerical and analytical methods were used to estimate the energy loss of the hydraulic jump in the conduit. The E_1 and E_2 were used for energy before and after the hydraulic jump, respectively and the energy loss ratio is shown by $\Delta E/E_2$ (Table 7). Three slopes of 0.00, 0.01 and 0.02 with different Froude numbers were used to evaluate energy loss. Variation of the energy loss ratio in terms of both Froude number and length ratio (L_r/d_1) is shown in Figure 9. The numerical and analytical results indicate that the energy loss ratio increases with increasing the Froude number (Figure 9a). In the slope of 0.00, the energy loss increases by 16% with increasing the Froude number from 4.617 to 5.562 while this value is 23% and 22% for slopes of 0.01 and 0.02, respectively. Similar results were reported by previous researchers (Pourabdollah et al. 2019; Gupta et al. 2013). Figure 9b shows that the length of the jump increases with increasing the Froude number which leads to raising turbulence. Due to turbulence on the upper surface of the hydraulic jump, several rollers can be formed in the mixing layer which increases the energy loss. Therefore, more rollers form with increasing the length of the hydraulic jump which leads to more energy loss. As shown in Table 7, for the 0.0 slope, the length ratio (Lr / d1) increases by 20% with increasing the Froude number from 4.617 to 5.562. This value is 26% and 20% for the slopes of

0.01 and 0.02, respectively. Table 8 shows that by changing both the Froude number from 4.0 to 6.0 and the slope from 0.00 to 0.02, the length ratio in the closed conduit can be increased by 58%.

1.1. Determination of Sequent Depths

As shown in the last section, the hydraulic jump parameters such as L_r, d_1, d_2, d_3, and d_4 are a function of flow depth (d_1), Froude number (Fr), slope (S_0) and conduit (D). Then the following equation can be developed using dimensional analysis:

$$\frac{d_4}{d_1} \text{ and } \frac{d_3}{d_1} \text{ and } \frac{d_2}{d_1} \text{ and } \frac{L_r}{d_1} = f\left(Fr_1, \frac{d_1}{D}, S_0\right) \tag{32}$$

To develop the relationship between the parameters in the hydraulic jump in the above equation, the presented analytical method (equations 7 to 31) was used to generate 3377 data sets. To generate the data, some initial information such as Fr_1, d_1, D and S_0 was taken from the research of Ezzeldin et al. (2000a). In the next step, the equations of (7) to (31) and the trial and error method were used to determine other parameters. The range of generated data is shown in Table 8. The equations suggested in the present study are valid for input parameters in ranges of $0.2 \le d_1/D \le 0.35$, $4.0 \le Fr_1 \le 6.0$ and $0 \le S_0 \le 0.02$. As shown in Table 9, several equations were developed to predict the flow depth in a closed conduit and the hydraulic jump length. The results are compared with the equations recommended by Ezzeldin et al. (2000a) and Negm (2003). Out of 3377 data sets, 80% of data was selected for training and the rest of the data (20%) was chosen for testing. The range of data employed by Ezzeldin et al. (2000a) was approximately similar to this study, while the equation proposed by Negm (2003) is valid in the range of $0.21 \le d_1/D \le 0.35$, $4.0 \le Fr_1 \le 6.0$ and $-0.02 \le S_0 \le 0.02$. To predict d_4/d_1, the highest accuracy belongs to the equation suggested in the present study with R^2=0.992, MAE=0.085 and RMSE=0.105. It should be mentioned that the accuracy of the equation developed by Negm (2003) with R^2=0.978, MAE=0.21 and RMSE=0.254 is higher than Ezzeldin et al. (2000a) and this equation can be used for both negative and positive slope. Although the equation of L_r/d_1 provides the lowest accuracy (R^2=0.966, MAE=0.557 and RMSE=0.684), the results are very appropriate and acceptable to predict hydraulic jump. The results show that the accuracy of d_3/d_1 is higher than d_2/d_1 (R^2=0.984, MAE=0.172, and RMSE=0.203). A comparison between generated data by analytical method and predicted data is shown in Figure 10. Although the best fit belongs to d_4/d_1, other graphs also show that the recommended equations are able to predict the hydraulic jump parameters with high accuracy ,then they can be easily used in practical proposed.

Conclusions

The supercritical flow is the main reason for local scour and sediment erosion at the culvert outlet. To protect the channel against erosion, the hydraulic jump has been often used as an economical alternative to dissipate energy in conduit and culvert design. In this research, analytical and numerical methods were employed to study hydraulic jump characteristics in a conduit. Three slopes of 0.00, 0.01, and 0.02 were used to determine the effect of a positive slope on the hydraulic jump. The numerical and analytical models were validated using the experimental results. Results indicate that the numerical method is able to predict the flow depth in hydraulic jump with higher accuracy (R^2=0.991, RMSE=0.077) in comparison with the analytical method (R^2=0.881, RMSE=0.291). The numerical and analytical results indicate that the energy loss ratio and sequence depth increase with increasing Froude number. An average increase of both d_2/d_1 and d_3/d_1 is around 15% with increasing the slope from 0.00 to 0.02 and Froude number from 4.61 to

5.56. Furthermore, in the slope of 0.00, the energy loss increases by 16% with increasing the Froude number from 4.617 to 5.562 while this value is 23% and 22% for slopes of 0.01 and 0.02, respectively. Several equations were developed for the prediction of hydraulic jump characteristics in terms of Fr_1, S_0 and conduit depth (D). Although the best fit belongs to d_4/d_1, other graphs also show that the recommended equations are able to predict the hydraulic jump parameters with high accuracy ,then they can be easily used in practical proposed.

Conflicts of Interest: None

References

Abbaspour, A.; Farsadizadeh, D.; Hosseinadeh, A.D.; Sadraddini, A.A. 2009. Numerical study of hydraulic jumps on corrugated beds using turbulence models. Turk. J. Eng. Environ. Sci. 2009, 33, 61–72.

Abdel-Mageed NB. 2015. Effect of channel slope on hydraulic jump characteristics. Phys Sci Int J 7(4):223–233.

Altalib, A. N., Mohammed, A. Y. & Hayawi, H. A. 2019. Hydraulic jump and energy dissipation downstream stepped weir. Flow Measurement and Instrumentation, 69, 101616.

Azimi, H., Shabanlou, S. & Salimi, M. S. 2014. Free surface and velocity field in a circular channel along the side weir in supercritical flow conditions. Flow Measurement and Instrumentation, 38, 108-115.

Babaali, H., Shamsai, A. & Vosoughifar, H. 2015. Computational Modeling of the Hydraulic Jump in the Stilling Basin with Convergence Walls Using CFD Codes. Arabian Journal for Science and Engineering, 40**,** 381-395.

Baharvand, S., Jozaghi, A., Fatahi-Alkouhi, R., Karimzadeh, S., Nasiri, R. & Lashkar-Ara, B. 2020. Comparative Study on the Machine Learning and Regression-Based Approaches to Predict the Hydraulic Jump Sequent Depth Ratio. Iranian Journal of Science and Technology, Transactions of Civil Engineering.

Bayon, A., Lopez-Jimenez, P.A., 2015. Numerical analysis of hydraulic jumps using OpenFOAM. J. Hydroinformatics 17 (4), 662e678.

Bayon, A., Macián-Pérez, J., Valles-Morán, F. & López-Jiménez, P. 2019. Effect of RANS turbulence model in hydraulic jump CFD simulations.

Bayon, A., Valero, D., García-Bartual, R., Vallés-Morán, F. J. & López-Jiménez, P. A. 2016. Performance assessment of OpenFOAM and FLOW-3D in the numerical modeling of a low Reynolds number hydraulic jump. Environmental Modelling & Software, 80**,** 322-335.

Beirami, M. K. & Chamani, M. R. 2006. Hydraulic Jumps in Sloping Channels: Sequent Depth Ratio. Journal of Hydraulic Engineering, 132, 1061-1068.

Beirami, M. & Chamani, M. 2010. Hydraulic jump in sloping channels: roller length and energy loss. Canadian Journal of Civil Engineering, 37, 535-543.

Caric, D. M. 1977. "Flow in circular conduits." Water Power Dam Constr., 29(11), 29–33.

Carvalho, R., Lemos, C., Ramos, C., 2008. Numerical computation of the flow in hydraulic jump stilling basins. J. Hydraulic Res. 46 (6), 739e752.

Celik, I.B., Ghia, U., Roache, P.J., 2008. Procedure for estimation and reporting of uncertainty due to discretization in CFD applications. ASME J. Fluids Eng. 130 (7), 1e4.

Chanson, H. 2015. Energy dissipation in hydraulic structures, CRC Press.

Chiew, Y. & Emadzadeh, A. (2017) Experimental investigation of free surface dynamics and pressure fluctuations in a closed-conduit hydraulic jump. E-proceedings of the 37th IAHR World Congress. IAHR Kuala Lumpur, Malaysia.

Chippada, S.; Ramaswamy, B.; Wheeler, M.F. Numerical simulation of hydraulic jump. Int. J. Numer. Meth. Eng. 1994, 37, 1381–1397.

Chow Ven Te. Open channel hydraulics. New York (NY): McGraw-Hill Book Co. Inc.; 1959.

Daneshfaraz, R., Majediasl, M., Mirzaee, R. & Tayfur, G. 2020. Hydraulic jump in a rough sudden symmetric expansion channel. AUT Journal of Civil Engineering. DOI: 10.22060/AJCE.2020.18227.5667.

De Padova, D.; Mossa, M.; Sibilla, S.; Torti, E. 3D SPH modeling of hydraulic jump in a very large channel.J. Hydraul. Res. 2010, 51, 158–173.

Ebrahimi, S.; Salmasi, F.; Abbaspour, A. Numerical Study of Hydraulic Jump on Rough Beds Stilling Basins. J. Civ. Eng. Urban. 2013, 3, 19–24.

Ezzeldin, M.M., Negm, A.M., and Attia, M.I. 2000a. "Experimental Investigation on the Hydraulic Jump in Sloping Rectangular Closed Conduits", Alex. Eng. Journal, Faculty of Eng., Alex. Univ., Egypt, Vol. 39, No. 5, pp. 763-775.

Ezzeldin, M.M., Negm, A.M., And Attia, M.I. 2000b. "Experimental Investigation on the Hydraulic Jump in Adversely Sloping Rectangular Closed Conduits", Alex. Eng. Journal, Faculty of Eng., Alex. Univ., Egypt, Vol. 39, No. 5, , pp. 751- 762.

Godley, A. 2002. Flow measurement in partially filled closed conduits. Flow Measurement and Instrumentation, 13, 197-201.

Gonzalez, A. and Bombardelli, F., Two-Phase Flow Theory and Numerical Models for Hydraulic Jumps, Including Air Entrainment, in Proc. XXXI IAHR Congress, Seoul, Korea, 2005.

Haindl, K. (1957). "Hydraulic Jumps in Closed Conduits." Proceedings of the International Association for Hydraulic Research, Delft, Holland, D32-1 to D32-12.

Hager, W. H. 1999. Wastewater hydraulics, Springer-Verlag, Berlin.

Hager, W. H. 1988. “B-Jump in sloping channel.” J. Hydraul. Res., 26-5, 539–558.

Hager, W.H., B-jump in Sloping Channel, Journal of Hydraulic Research, Vol. 26, No. 5, 1988,

Hager, W.H.; Bremen, R. 1989, Classical hydraulic jump: Sequent depths. J. Hydraul. Res. 27, 565–585.

Hager, W. H. (1992). Energy Dissipators and Hydraulic Jump. Kluwer Academic Publishers, Dordrecht, The Netherlands.

Harada, S.; Li, S.S. 2018. Modeling hydraulic jump using the bubbly two-phase flow method. Environ. Fluid Mech., 18, 335–356.

Hafnaoui, M. A. & Debabeche, M. 2020. Numerical modeling of the hydraulic jump location using 2D Iber software. Modeling Earth Systems and Environment.

Hotchkiss, R. H. & Larson, E. A. 2005. Simple methods for energy dissipation at culvert outlets. Impacts of Global Climate Change.

Hotchkiss, R. H., Flanagan, P. J., and Donahoo, K. 2003. Hydraulic jumps in broken-back culverts. Transportation Research Record 1851, Transportation Research Board, Washington, DC, 35–44.

Hsu, S. T., Wang, J. S., and Elder, R. A. (1980). "Hydraulic Designs of Open-Channel Flows in Circular Conduits." International Conference on Water Resources Development, Taipei, Taiwan, 1019-1031.

Harun, M. A., Ab. Ghani, A., Mohammadpour, R. & Chan, N. W. 2021. GEP- and MLR-based equations for stable channel analysis. Journal of Hydroinformatics. DOI: 10.2166/hydro.2021.047

Gupta, S. K., Mehta, R. C. & Dwivedi, V. K. 2013. Modeling of Relative Length and Relative Energy Loss of Free Hydraulic Jump in Horizontal Prismatic Channel. Procedia Engineering, 51, 529-537.

Jaypragasam, R. 1987. Design Criteria for Stability of Stilling Basins Based on Model Studies, Intl. Symposium on New Technology Model Testing in Hydraulic Research, Pune, India, pp. 115-120.

Kateb, S., Debabeche, M. & Riguet, F. 2015. Hydraulic Jump in a Sloped Trapezoidal Channel. Energy Procedia, 74, 251-257.

Quraishi, A. A. & Al-Brahim, A. M. 1992. Hydraulic jump in sloping channel with positive or negative step. Journal of Hydraulic Research, 30, 769-782.

Kawagoshi, N., Hager, W.H. 1990. B-jump in sloping channel II. J. Hydraul. Res., 28(2), 235–252.

Kindsvater, C.E. 1944. The hydraulic jump in sloping channels. Trans. ASCE, 109, 1107–1154.

Kumar M, Lodhi AS. 201. Hydraulic jump over sloping rough floors. ISH J Hydraul Eng 22(2):127–134.

Kumar, M., Mishra, N. & Kumar, S. 2021. Investigation of Hydraulic Jump Over Rough Sloping Floor in Prismatic Rectangular Channel—An Experimental Study. Springer Singapore, 221-231.

Li, X., Jin, L., Engel, B. A., Yang, Z., Wang, W., He, W. & Wang, Y. 2020. Influence of the structure of cylindrical mobile flumes on hydraulic performance characteristics in U-shaped channels. Flow Measurement and Instrumentation, 72, 101708.

Long, D., Steffler, P. M. & Rajaratnam, N. 1991. A numerical study of submerged hydraulic jumps. *Journal of Hydraulic Research*, 29**,** 293-308.

Lowe, N. J., Hotchkiss, R. H. & Nelson, E. J. 2011. Theoretical determination of sequent depths in closed conduits. Journal of irrigation and drainage engineering, 137, 801-810.

Ma, J.; Oberai, A.A.; Lahey, R.T.; Drew, D.A. Modeling air entrainment and transport in a hydraulic jump using two-fluid RANS and DES turbulence models. Heat Mass Transf. 2011, 47, 911.

Madsen, P.A.; Simonsen, H.J.; Pan, C.H. 2005. Numerical simulation of tidal bores and hydraulic jumps. Coast. Eng.,52, 409–433. Meth. Eng. 37, 1381–1397.

Mohammadpour, R., Ghani, A. A. & Azamathulla, H. M. 2013. Numerical modeling of 3-D flow on porous broad crested weirs. *Applied Mathematical Modelling*, 37**,** 9324-9337.

Mohammadpour, R., Sabzevari, T. & Mohammadpour, F. 2014. Investigation of Local Scour development around Abutment by using Experimental and Numerical Models. *Caspian Journal of Applied Science Research*, 3, 1-11.

Mohammadpour, R. 2017. Prediction of local scour around complex piers using GEP and M5-Tree. *Arabian Journal of Geosciences*, 10, 416.

Mohammadpour, R., Asaie, Z., Shojaeian, M. R. & Sadeghzadeh, M. 2018. A hybrid of ANN and CLA to predict rainfall. *Arabian Journal of Geosciences*, 11, 533.

Montes, S. 1998. Hydraulics of open-channel flow, ASCE, Reston, VA.

Rajaratnam, N. 1965. Hydraulic jump in horizontal conduits. Water Power Dam Constr., 17(2), 80–83.

Rajaratnam N, Subramanya K. Profile of hydraulic jump. Journal of Hydraulic Division. ASCE. 1968;94(3):663–673.

Najafzadeh, M. 2019. Evaluation of conjugate depths of hydraulic jump in circular pipes using evolutionary computing. Soft Computing, 23, 13375-13391.

Negm, A.A. M. 2003. Analysis And Formulation Of Hydraulic Jumps In Sloping Rectangular Closed Conduits. Seventh International Water Technology Conference Egypt 1-3.

Ohtsu, I., Yasuda, Y. 1991. Hydraulic jump in sloping channels. J. Hydraul. Eng., 117(7), 905–921.

Pagliara, S.; Palermo, M. 2015. Hydraulic jumps on rough and smooth beds: Aggregate approach for horizontal and adverse-sloped beds. J. Hydraul. Res., 53, 243–252.

Palermo, M. & Pagliara, S. 2017. A review of hydraulic jump properties on both smooth and rough beds in sloping and adverse channels. Acta Scientiarum Polonorum. Formatio Circumiectus, 16**,** 91.

Palermo, M., and Pagliara, S. (2017). D-jump in rough sloping channels at low Froude numbers. Journal of Hydro-Environment Research, 14, 150-156.

Palermo, M., and Pagliara, S. (2018). Semi-theoretical approach for energy dissipation estimation at hydraulic jumps in rough sloped channels. Journal of Hydraulic Research, 56(6), 786-795.

Parsamehr P, Farsadizadeh D, Hosseinzadeh Dalir A, Abbaspour A, Nasr Esfahani MJ. 2017. Characteristics of hydraulic jump on rough bed with adverse slope. Hydraul Eng, ISH J.

Passandideh-Fard, M., Teymourtash, A. R. & Khavari, M. 2011. Numerical study of circular hydraulic jump using volume-of-fluid method. Journal of Fluids Engineering, 133, 011401.

Pham, Q. B., Mohammadpour, R., Linh, N. T. T., Mohajane, M., Pourjasem, A., Sammen, S. S., Anh, D. T. & Nam, V. T. 2021. Application of soft computing to predict water quality in wetland. Environmental Science and Pollution Research, 28, 185-200.

Pourabdollah, N., Heidarpour, M. & Abedi Koupai, J. 2019. An Experimental and Analytical Study of a Hydraulic Jump Over a Rough Bed with an Adverse Slope and a Positive Step. Iranian Journal of Science and Technology, Transactions of Civil Engineering, 43, 551-561.

Rashwan, I. M. H. 2013. A-jump in horizontal inverted semicircular open channels. *Ain Shams Engineering Journal,* 4**,** 585-592.

Raikar, R. V., Shiva Reddy, M. S. & Vishwanadh, G. K. 2010. Normal and critical depth computations for egg-shaped conduit sections. Flow Measurement and Instrumentation, 21, 367-372.

Rajaratnam, N. (1967). “Hydraulic jumps.” Advances in hydroscience, V.T. Chow, ed., Vol. 4, Academic Press, New York, NY, 197–280.

RangaRaju, K.G. (1993). Flow through open channels, Tata McGraw Hills, New Delhi, 196–198.

Rostami, F., Shahrokhi, M., Md Saod, M. A. & Sabbagh Yazdi, S. R. 2013. RETRACTED: Numerical simulation of undular hydraulic jump on smooth bed using volume of fluid method. *Applied Mathematical Modelling,* 37**,** 1514-1522.

Smith, C. D. & Chen, W. 1989. The hydraulic jump in a steeply sloping square conduit. Journal of Hydraulic Research, 27, 385-399.

Subramanya, K., Flow in Open Channels, McGraw-Hill Publishing Co. Ltd., New Delhi, 1986.

Teymourtash, A. R. & Khavari, M. 2011. Numerical Study of Circular Hydraulic Jump Using Volume-of-Fluid Method. Journal of Fluids Engineering, 133, 011401-1.

Thompson, P. L., and Kilgore, R. T. 2006. Hydraulic jump.” Hydraulic Engineering Series No. 14, Hydraulic design of energy dissipators for culverts and channels, 3rd Ed., Federal Highway Administration,Washington, DC, 6-1–6-14.

Valero, D.; Bung, D.B.; Crookston, B.M. Energy dissipation of a Type III basin under design and adverse conditions for stepped and smooth spillways. J. Hydraulic Eng. 2018, 144, 04018036.

Viti, N., Valero, D. & Gualtieri, C. 2018. Numerical Simulation of Hydraulic Jumps. Part 2: Recent Results and Future Outlook. Water, 11, 28.

Wang, Chunli; Li, S. S. 2018. "Hydraulic Jump and Resultant Flow Choking in a Circular Sewer Pipe of Steep Slope" *Water* 10, no. 11: 1674.

Wang, K., Tang, R., Bai, R. & Wang, H. 2021. Evaluating phase-detection-based approaches for interfacial velocity and turbulence intensity estimation in a highly-aerated hydraulic jump. Flow Measurement and Instrumentation, 81, 102045.

Wang, S., Wang, D., Niu, P., Wei, P. & Liu, M. 2017. Mass flowrate measurement using the swirl motion in circular conduits. Flow Measurement and Instrumentation, 54, 177-184.

Witt, A., Gulliver, J. & Shen, L. 2015. Simulating air entrainment and vortex dynamics in a hydraulic jump. International Journal of Multiphase Flow, 72, 165-180.

Witt, A.; Gulliver, J.; Shen, L. 2018. Numerical investigation of vorticity and bubble clustering in an air entraining hydraulic jump. Comput. Fluids, 172, 162–180.

Yokoi K, Xiao F. 1999. A numerical study of the transition in the circular hydraulic jump. Phys Lett A 257:153–157.

Zhao, Q., Misra, S. K., Svendsen, I. A. & Kirby, J. T. 2004 Numerical study of a turbulent hydraulic jump. Proc. 17th Engrng. Mech. Div. Conf, Citeseer.

Zounemat-Kermani, M., Rajaee, T., Ramezani-Charmahineh, A. & Adamowski, J. F. 2017. Estimating the aeration coefficient and air demand in bottom outlet conduits of dams using GEP and decision tree methods. Flow Measurement and Instrumentation, 54, 9-19.

List of Figures

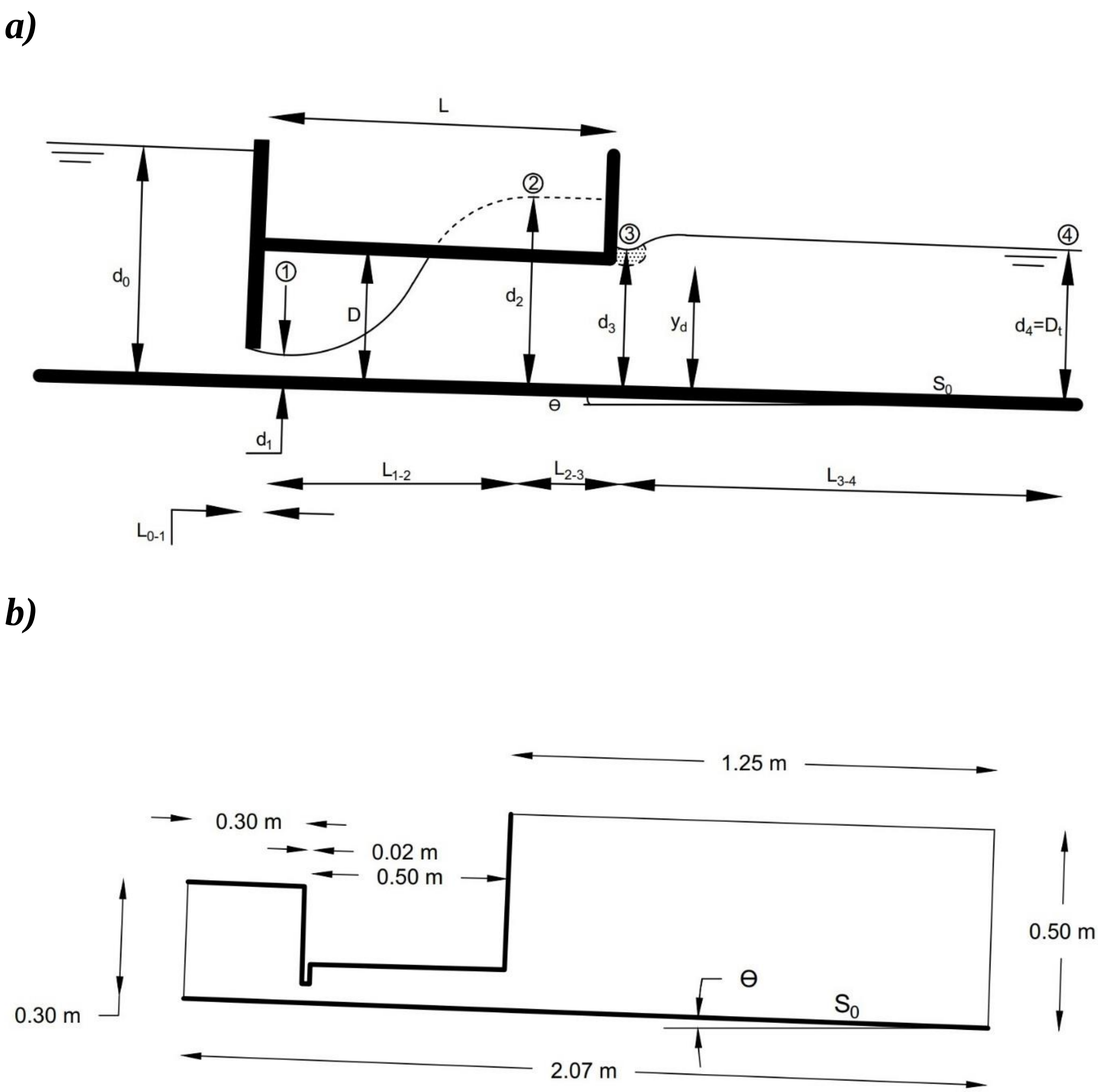

Figure 1: Channel for hydraulic jump in conduit

a) Parameters of hydraulic jump; b) Channel dimension in numerical modeling *a)*

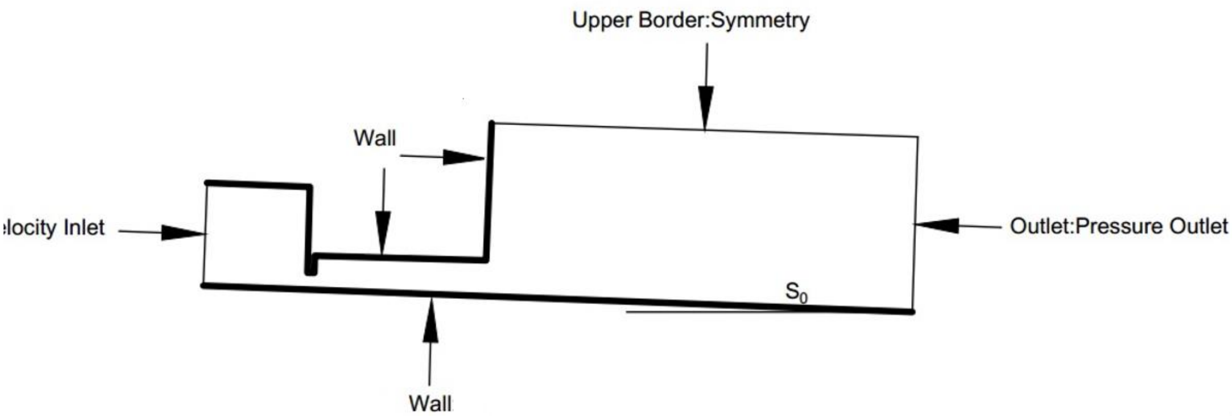

b)

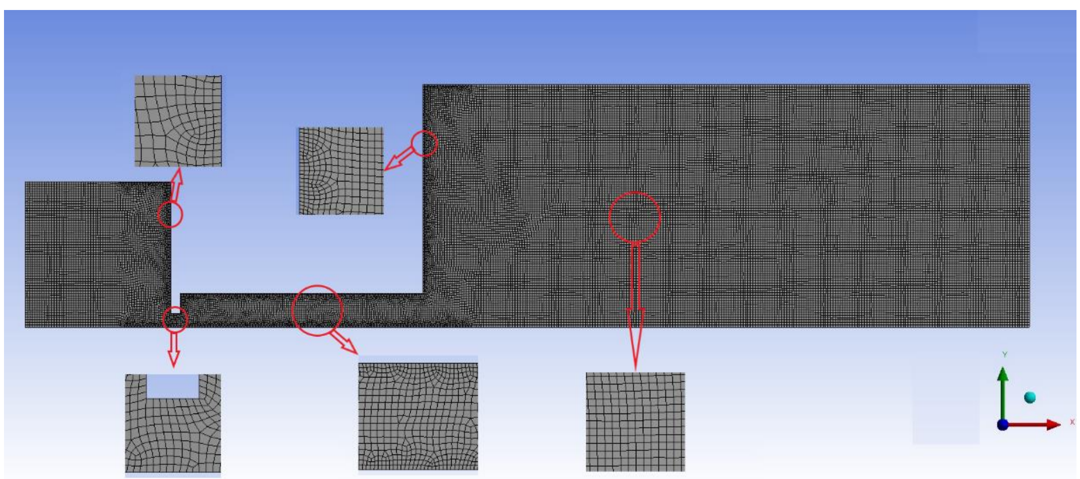

Figure 2: Channel in numerical modelling

a) Boundary condition; b) structural meshes for simulation

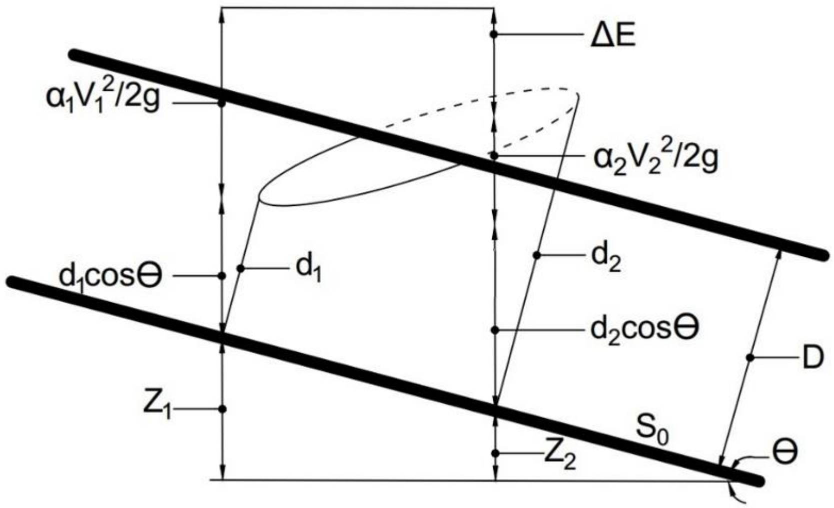

Figure 3: Sketch of energy loss due to the hydraulic jump in conduit

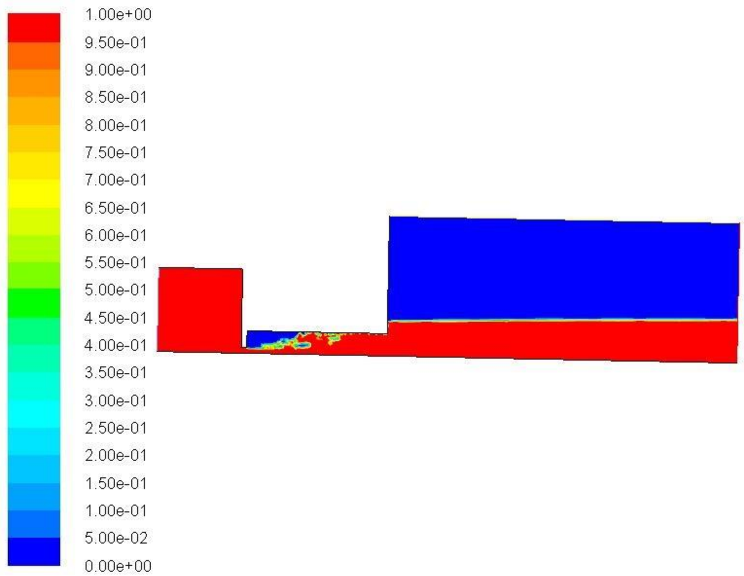

Figure 4: Hydraulic jump using numerical modelling

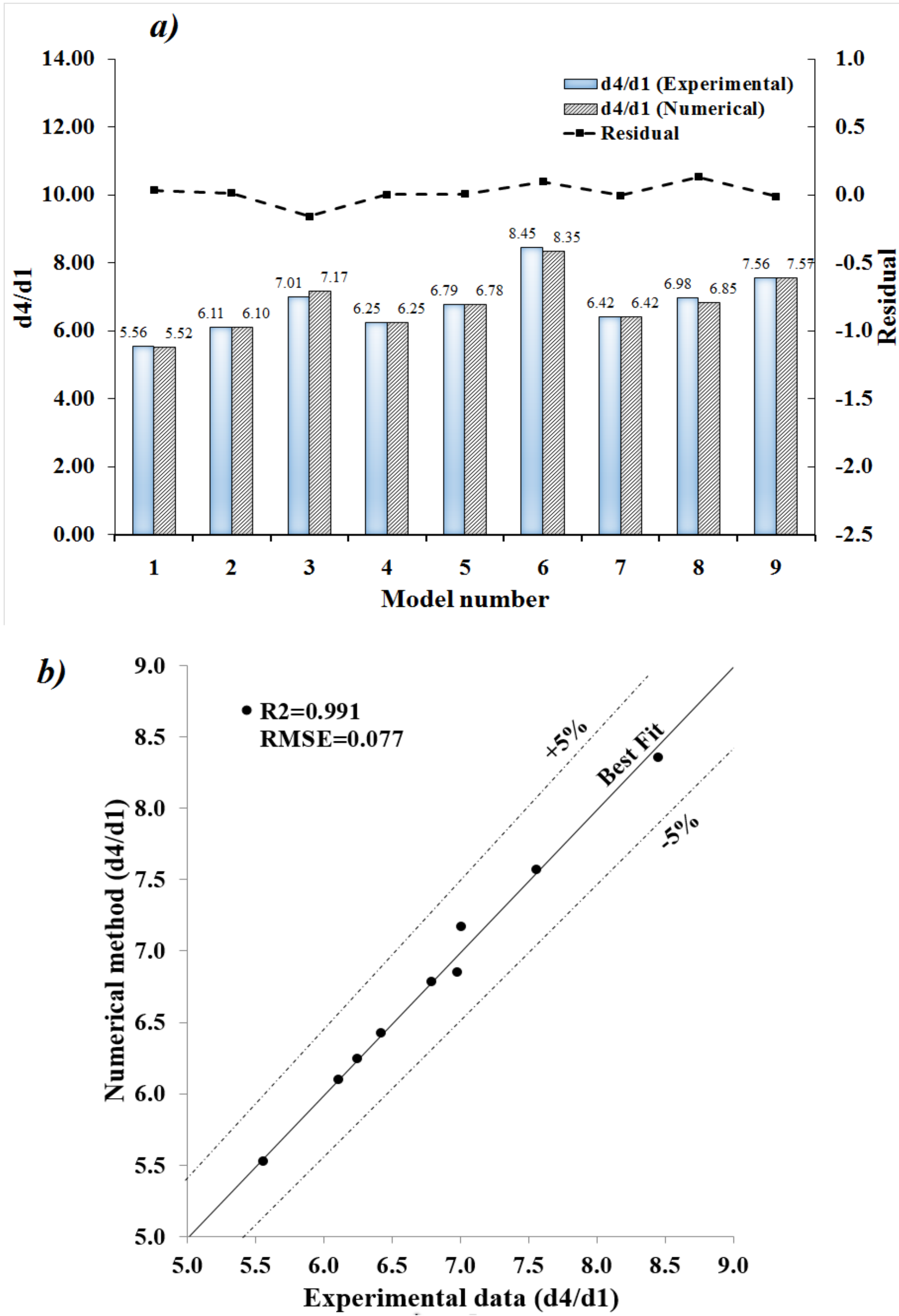

Figure 5: A comparison between numerical method and experimental data given by Ezzeldin et al. (2000a); a) bar chart and residual graph; b) scatter graph

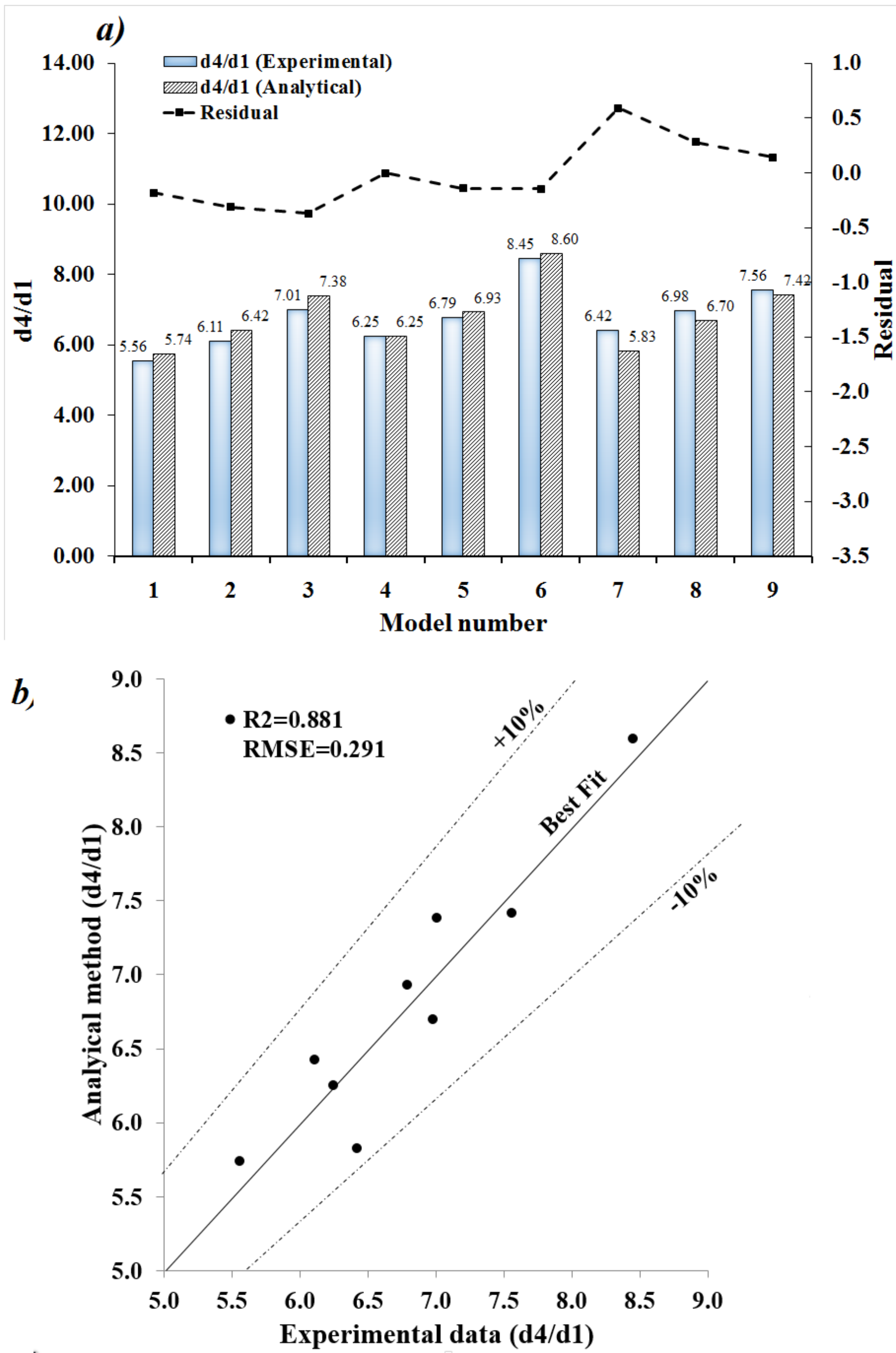

Figure 6: A comparison between analytical method and experimental data given by Ezzeldin et al. (2000); a) bar chart and residual graph; b) scatter graph

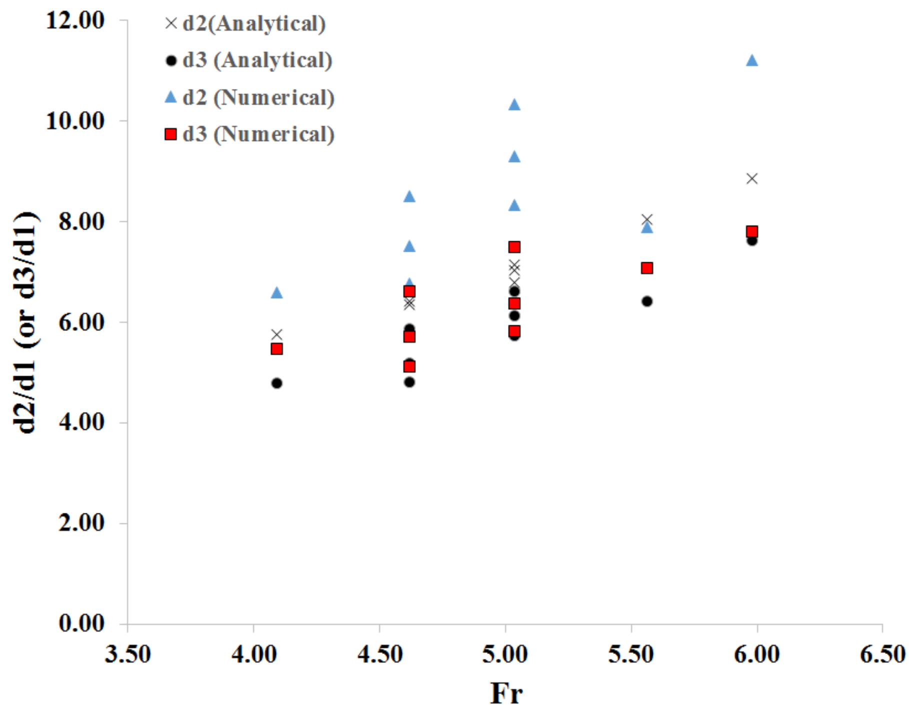

Figure 7: Variation of the flow depth after the hydraulic jump in terms of Froude number

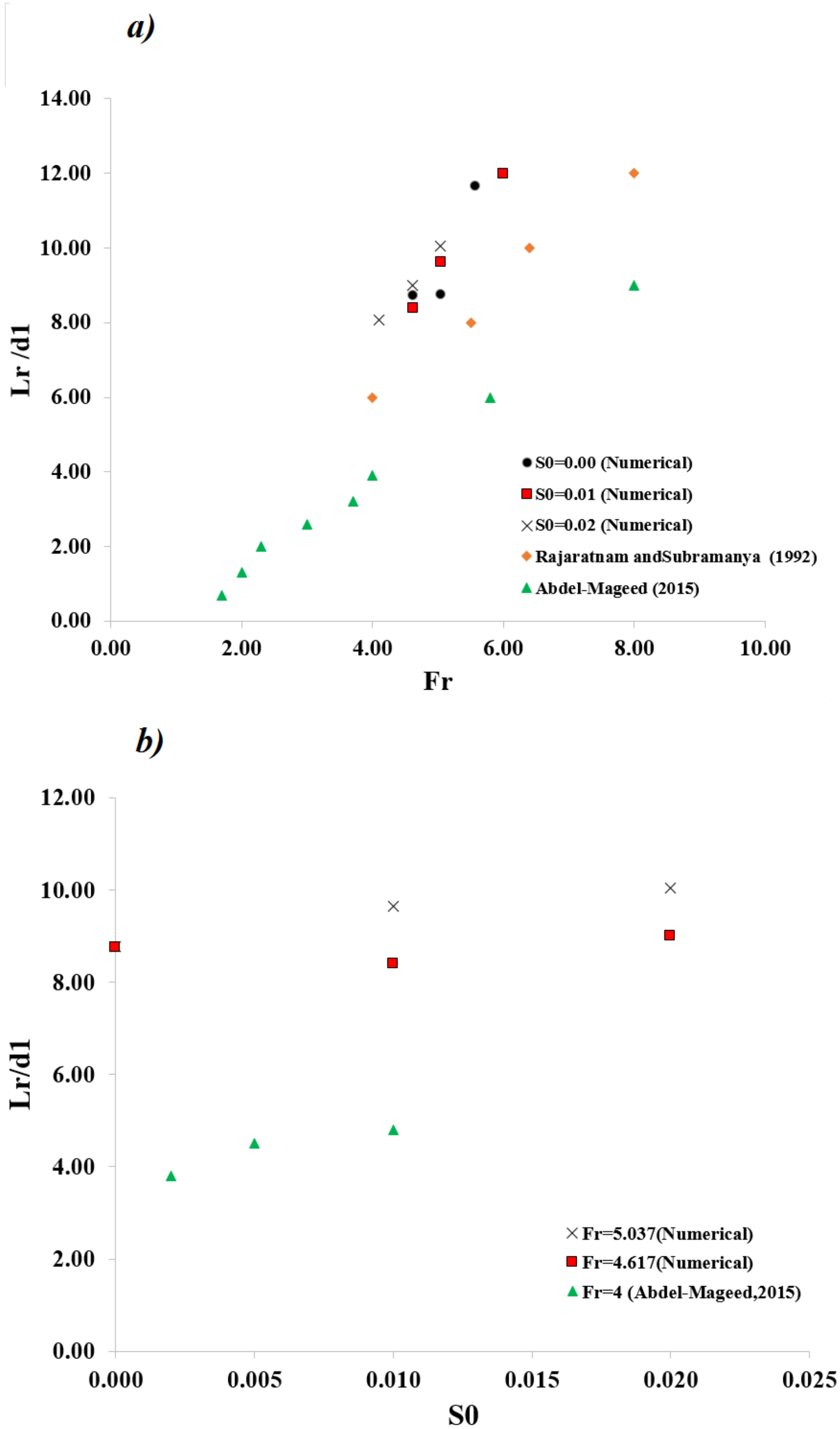
a)
14.00
12.00
10.00
8.00
6.00
4.00
2.00
0.00
Lr /d1
0.00
2.00
4.00
6.00
8.00
10.00
Fr
S0=0.00 (Numerical)
S0=0.01 (Numerical)
S0=0.02 (Numerical)
Rajaratnam andSubramanya (1992)
Abdel-Mageed (2015)
b)
12.00
10.00
8.00
6.00
4.00
2.00
0.00
Lr/d1
0.000
0.005
0.010
0.015
0.020
0.025
S0
Fr=5.037(Numerical)
Fr=4.617(Numerical)
Fr=4 (Abdel-Mageed,2015)

Figure 8: Variation of hydraulic jump length in terms of a) Froude number; b) Slope

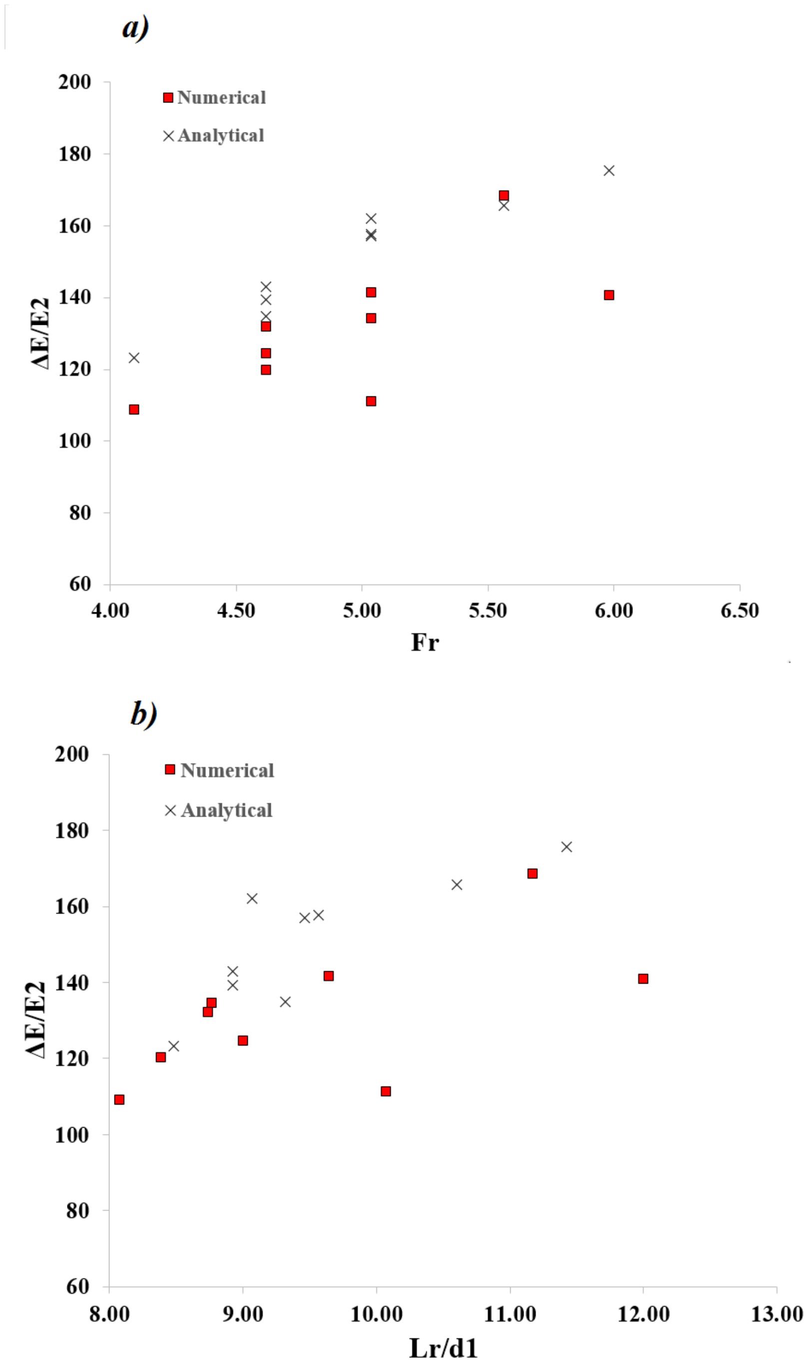

Figure 9: Variation of the energy loss ratio in terms of a) Froude number; b) Jump length ratio

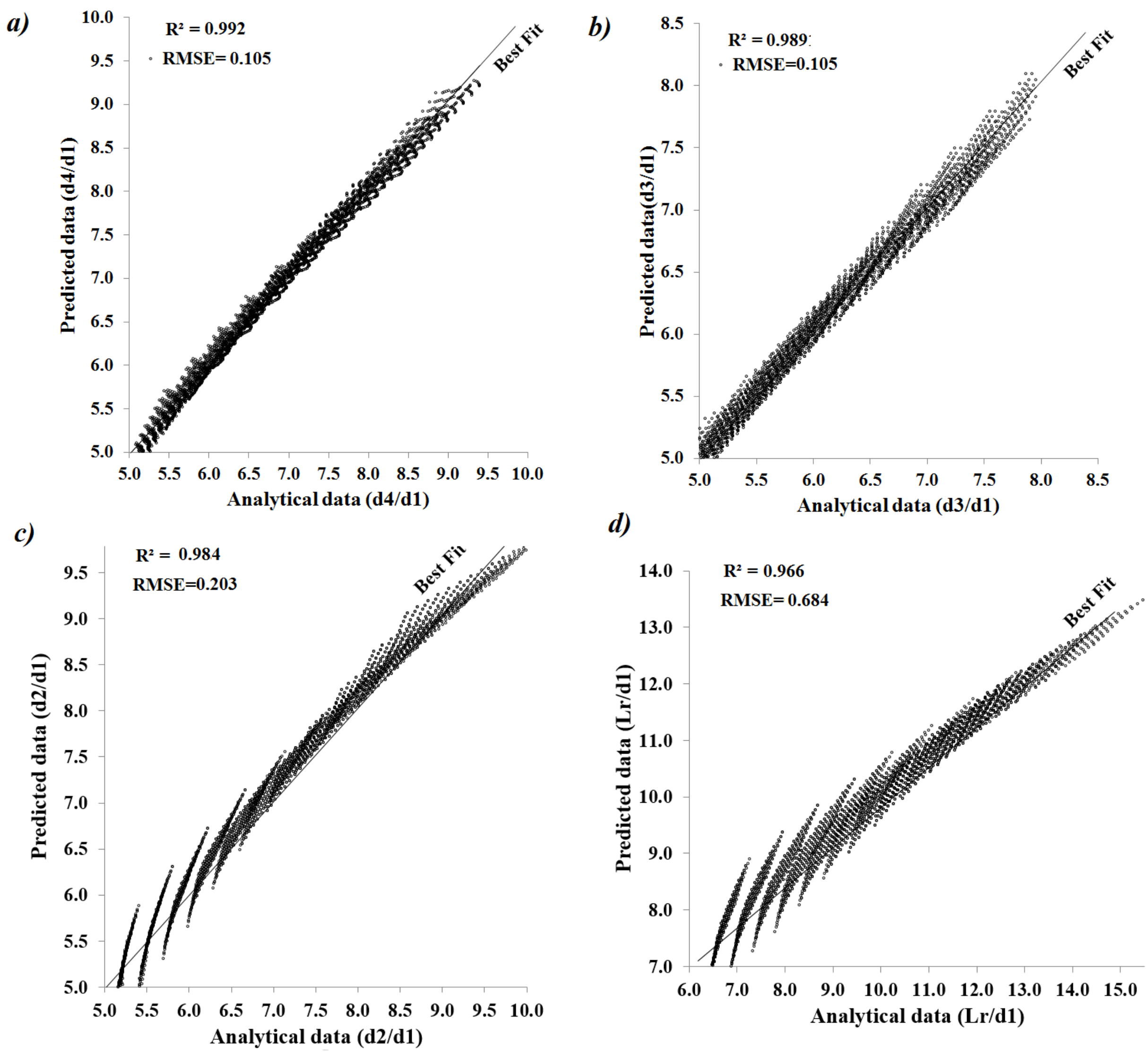

Figure 10: A comparison between analytical and predicted data a) d_4/d_1 ;b) d_3/d_1 ;c) d_2/d_1 ;d) L_r/d_1

Table 1: A summary of numerical studies of hydraulic jumps

Autor(s)	**Approach**	**Turbulence model(s)**
Long et al. (1991)	RANS	*k*-*ε*
Chippada et al. (1994)	RANS	STD k −ε
Zhao et al. (2004)	RANS	STD k –ε; Multi-scale (k –l)
Gonzalez and Bombardelli (2005)	RANS	STD k −ε
Carvalho et al. (2008)	RANS	RNG k −ε
Abbaspour et al. (2009)	RANS	STD k −ε; RNG k −ε
Ma et al. (2011)	RANS	k −ω
Ebrahimi et al. (2013)	RANS	STD k −ε
Rostami et al. (2013)	RANS	RNG k-ε
Bayon-Barrachina and Jiménez (2015)	RANS	STD k −e; RNG k −e; k −ω
Witt et al. (2015)	RANS	realizable k −ε
Babaali et al. (2015)	RANS	STD k-ε; RNG k-ε
Bayon et al. (2016)	RANS	RNG k −ε
Witt et al. (2018)	RANS	realizable k −ε
Harada and Li (2018)	RANS	k −ε, k −ω
Valero et al. (2018)	RANS	RNG k −ε

Table 2: Name of parameters in conduit

Character(s)	Explanation
S_0	channel slope
Fr_1	Froude number in cross-section (1)
d_1,d_2,d_3 and d_4(D_t)	flow depth in section 1,2,3 and 4
D	conduit depth
y_d	flow depth immediately after conduit
θ	Channel slope.
W	flow depth after the gate (=0.58 d1)
L_{0-1}	distance between gate and section (1)
$L_r = L_{1-2}$	hydraulic jump length= distance between section (1) and (2)
L_{2-3}	distance between section (2) and (3)
L_{3-4}	distance between section (3) and (4)
B	Channel width

Table 3: The experimental results (Ezzeldin et al., 2000) was used in numerical modeling

S_0	Fr_1	d_1/D	d_4/d_1
0	4.617	0.3	5.56
0	5.037	0.233	6.11
0	5.562	0.263	7.01
0.01	4.617	0.3	6.25
0.01	5.037	0.233	6.79
0.01	5.982	0.21	8.45
0.02	4.093	0.3	6.42
0.02	4.617	0.233	6.98
0.02	5.037	0.21	7.56

Table 4: Result of numerical modeling with the different slope of conduit

S_0	D (m)	Q (Lit/s)	Fr_1	d_1 (m)	d_2 (m)	d_3 (m)	d_4 (m)	L_r (m)	d_1/D	d_2/d_1	d_3/d_1	d_4/d_1
0.000	0.070	4.400	4.617	0.021	0.142	0.107	0.116	0.184	0.300	6.762	5.114	5.524
0.000	0.090	4.790	5.037	0.021	0.175	0.122	0.128	0.184	0.233	8.329	5.819	6.095
0.000	0.070	4.352	5.562	0.018	0.142	0.127	0.129	0.201	0.263	7.895	7.071	7.167
0.010	0.070	4.401	4.617	0.021	0.158	0.120	0.131	0.176	0.300	7.527	5.718	6.247
0.010	0.090	4.791	5.037	0.021	0.195	0.134	0.142	0.203	0.233	9.303	6.370	6.782
0.010	0.080	4.080	5.982	0.017	0.191	0.133	0.142	0.204	0.213	11.227	7.796	8.353
0.020	0.070	3.901	4.093	0.021	0.138	0.115	0.135	0.170	0.300	6.593	5.473	6.422
0.020	0.080	3.680	4.617	0.019	0.162	0.126	0.130	0.171	0.238	8.510	6.607	6.847
0.020	0.100	4.801	5.037	0.021	0.217	0.157	0.159	0.211	0.210	10.334	7.492	7.571

Table 5: Depth ration of d4/d1in conduit using numerical, experimental given by Ezzeldin et al. (2000a) and analytical methods

No.	S_0	Fr_1	**d1/D**	d_4/d_1			**Comparison Between Experimental and Numerical method**		**Comparison Between Experimental and Analytical method**	
				Num.	**Exp.**	**Ana.**	**Residual (d_4/d_1)**	**Error (%)**	**Residual (d_4/d_1)**	**Error (%)**
1	0	4.617	0.300	5.52	5.56	5.74	0.036	0.65	-0.18	3.25
2	0	5.037	0.233	6.10	6.11	6.42	0.015	0.24	-0.31	5.09
3	0	5.562	0.233	7.17	7.01	7.38	-0.157	2.24	-0.37	5.31
4	0.01	4.617	0.300	6.25	6.25	6.25	0.003	0.05	0.00	0.03
5	0.01	5.037	0.233	6.78	6.79	6.93	0.008	0.11	-0.14	2.09
6	0.01	5.982	0.210	8.35	8.45	8.60	0.097	1.15	-0.15	1.73
7	0.02	4.093	0.300	6.42	6.42	5.83	-0.002	0.03	0.59	9.23
8	0.02	4.617	0.238	6.85	6.98	6.70	0.133	1.90	0.28	4.05
9	0.02	5.037	0.210	7.57	7.56	7.42	-0.011	0.15	0.14	1.87

Table 6: Result of analytical method with different slope of conduit

S_0	D (m)	Q (Lit/s)	Fr_1	d_1 (m)	d_2 (m)	d_3 (m)	d_4 (m)	L_r (m)	d_1/D	d_2/d_1	d_3/d_1	d_4/d_1
0.000	0.070	4.400	4.617	0.021	0.133	0.101	0.121	0.187	0.300	6.36	4.81	5.74
0.000	0.090	4.790	5.037	0.021	0.143	0.121	0.135	0.190	0.233	6.79	5.74	6.42
0.000	0.070	4.352	5.562	0.018	0.145	0.116	0.133	0.191	0.257	8.04	6.42	7.38
0.010	0.070	4.401	4.617	0.021	0.139	0.109	0.131	0.196	0.300	6.60	5.19	6.25
0.010	0.090	4.791	5.037	0.021	0.148	0.129	0.146	0.199	0.233	7.03	6.13	6.93
0.010	0.080	4.080	5.982	0.017	0.151	0.130	0.146	0.194	0.213	8.87	7.63	8.60
0.020	0.070	3.901	4.093	0.021	0.121	0.101	0.122	0.178	0.300	5.75	4.80	5.83
0.020	0.080	3.680	4.617	0.019	0.122	0.111	0.127	0.170	0.238	6.43	5.86	6.70
0.020	0.100	4.801	5.037	0.021	0.150	0.139	0.156	0.201	0.210	7.14	6.62	7.42

Table 7: Determination of hydraulic jump energy in conduit

No.	S_0	Fr_1	Numerical Results						Analytical Results					
			L_r/d_1	ΔZ	E_1	E_2	ΔE	$\Delta E/E_2$	L_r/d_1	ΔZ	E_1	E_2	ΔE	$\Delta E/E_2$
1	0	4.617	8.743	0.000	21.561	0.162	21.399	132.0	6.355	0.000	21.561	0.154	21.407	139.4
2	0	5.037	8.774	0.000	25.622	0.189	25.432	134.3	6.790	0.000	25.622	0.157	25.465	162.2
3	0	5.562	11.172	0.000	27.423	0.162	27.261	168.5	8.042	0.000	27.423	0.164	27.258	165.7
4	0.01	4.617	8.393	0.002	21.560	0.178	21.384	120.0	6.598	0.002	21.560	0.159	21.403	134.9
5	0.01	5.037	9.650	0.002	25.620	0.180	25.443	141.5	7.033	0.002	25.620	0.162	25.460	157.0
6	0.01	5.982	12.006	0.002	28.943	0.204	28.741	140.8	8.866	0.002	28.943	0.164	28.781	175.5
7	0.02	4.093	8.078	0.003	16.946	0.154	16.795	108.9	5.749	0.004	16.946	0.137	16.813	123.1
8	0.02	4.617	9.007	0.003	19.135	0.152	18.986	124.5	6.428	0.003	19.135	0.133	19.005	143.0
9	0.02	5.037	10.078	0.003	25.653	0.229	25.428	111.2	7.136	0.004	25.653	0.162	25.496	157.8

Table 8: Statistical parameters of generated data using analytical method

	Fr_1	Fr_2	S_0	d_1/D	d_2/d_1	d_3/d_1	d_4/d_1	L_r/d_1
Minimum	4.000	0.404	0.000	0.200	5.122	3.859	4.839	6.385
Maximum	6.000	1.201	0.020	0.350	10.314	7.959	9.399	15.472
Mean	4.988	0.711	0.010	0.272	7.067	5.878	6.884	9.772
Standard Deviation	0.616	0.176	0.006	0.043	1.240	0.984	1.114	2.062
Count	3377	3377	3377	3377	3377	3377	3377	3377

Table 9: Recommended equations for hydraulic jump parameters

Equation		*Train Data*			*Test Data*		
		R^2	*MAE*	*RMSE*	R^2	*MAE*	*RMSE*
$\frac{d_4}{d_1}$=-2.807+1.784(Fr_1)+1.037$\left(\frac{d_1}{D}\right)$+51.075$(S_0)$	Present study	0.991	0.088	0.108	0.992	0.085	0.105
$\frac{d_3}{d_1}$=-0.7099+1.493(Fr_1)-4. 577$\left(\frac{d_1}{D}\right)$+38.0382$(S_0)$	Present study	0.989	0.087	0.107	0.989	0.085	0.105
$\frac{d_2}{d_1}$=-5.255+2.085(Fr_1)+6.613$\left(\frac{d_1}{D}\right)$+24.287$(S_0)$	Present study	0.983	0.173	0.204	0.984	0.172	0.203
$\frac{L_r}{d_1}$=-5. 775+2.358(Fr_1)+12. 697$\left(\frac{d_1}{D}\right)$+39.849$(S_0)$	Present study	0.9652	0.552	0.676	0.966	0.557	0.684
$\frac{d_4}{d_1} = 7.018-3.782(Fr_1)+1.573\left(Fr_1^{1.5}\right)+121.169\boldsymbol{S_0} \boldsymbol{- 2119.53S_0^2 + 0.5554}\left(\frac{d_1}{D}\right)$	Ezzeldin, et al. (2000a)	0.914	0.264	0.329	0.920	0.256	0.32
$\frac{d_4}{d_1} = 7.229-3.840(Fr_1)+1.596\left(Fr_1^{1.5}\right)+63.582\boldsymbol{S_0} \boldsymbol{- 489.914S_0^2 + 0.7665}\left(\frac{d_1}{D}\right)$	Negm (2003)	0.978	0.220	0.257	0.978	0.210	0.254